ROADSIDE PASSIVE MASW

Choon B. Park and Richard D. Miller
Kansas Geological Survey, The University of Kansas, Lawrence, Kansas, USA

Abstract

For the most accurate results, a 2D receiver array such as a cross or circular type should be used in a passive surface wave survey. It is often not possible to secure such a spacious area, however, especially if the survey has to take place in an urban area. A passive version of the multichannel analysis of surface waves (MASW) method is described that can be implemented with the conventional linear receiver array deployed alongside a road. Offline, instead of inline, nature of source points on the road is accounted for by a dispersion analysis scheme that tries to resolve azimuths of the responsible points by scanning through all possible incoming angles of 180 degrees. On the other hand, it is possible to account for cylindrical, instead of planar, nature of surface wave propagation that often occurs due to the proximity of source points by considering the distance between a receiver and a possible source point. Performance of the processing schemes is compared to that of the scheme that accounts for inline propagation only. Comparisons made with field data sets showed that the latter scheme can result in overestimation of phase velocities up to 30 percent, whereas the overestimation can be reduced to less than 10 percent if these natures are accounted for according to the proposed schemes.

Introduction

As the necessity of surveys inside urban areas grows and the active survey mode often does not achieve sufficient depth of investigation, the passive surface wave method utilizing those surface waves generated by local traffic is deemed to be a fascinating choice recently (Louie, 2001; Okada, 2003; Haruhiko and Hayashi, 2003; Yoon and Rix, 2004; Park et al., 2004). Furthermore, because the true 2D receiver array such as a cross layout is not a practical or possible mode of survey in urban areas populated with buildings, a method that can be implemented with the conventional 1D linear receiver array should get its own credit in any case (Louie, 2001). The underlying assumption with such a 1D method lies in the nature of wave propagation which is the same inline propagation as in the case of an active survey. Subsequent data processing for dispersion analysis is therefore a 1D scheme considering only those waves propagating parallel to (inline with) the linear receiver line.

In the case of a passive survey alongside a road, points of surface wave generation are usually on the road since waves are generated when moving vehicles travel onto irregularities on the road. Because the receiver line is always off the road, the wave propagation is therefore hardly in accordance with the inline propagation although being close to it when sources are at far distances. If those strong waves from nearby source points dominate and their offline nature is not accounted for during the dispersion analysis, phase velocities are overestimated approximately in inverse proportion to the cosine of the azimuth ($\cos\theta$). Furthermore, considering relatively strong energy from nearby source points, the dominating mode of propagation may be not only offline but also cylindrical with a wavefront whose curvature cannot be ignored.

Ways to account for these offline and cylindrical characteristics are described with results compared to those from the conventional analysis scheme based on the inline plane wave propagation. Fundamentals of data acquisition and processing techniques have evolved from the multichannel analysis of surface waves (MASW) method (Park et al., 1999) for active surface wave surveys. The

offline nature is accounted for by a scheme (Park et al., 2004) that scans through a possible range (180 degrees) of incoming azimuths of dominating waves for each frequency component of the dispersion analysis. The cylindrical nature is then accounted for by an additional scheme that calculates the approximate distance between a specific receiver and a possible source point determined from an examining azimuth and an approximate distance between the receiver line and the road. It is shown that these proposed schemes can correct for the overestimation to some degree but not completely, indicating that a true 2D array has to be used for the most accurate estimation. The incomplete correction becomes more significant for longer wavelengths. Tests with field data sets show the overestimation caused by the conventional inline processing can be as large as 30 percent, whereas the overestimation can be reduced to less than 10 percent by using the proposed schemes.

Roadside Passive Surface Waves

Three different types of wave propagation can exist: inline plane (IP), offline plane (OP), and offline cylindrical (OC) propagations (Figure 1). Propagation of waves generated from distant points on the surveying road (for example, at a distance 10 times or more array lengths) can be an example of the IP type if the road is fairly straight in the corresponding segment (Figure 1a). On the other hand, if the road turns or there are other roads around the surveying area, there can be waves generated at far distances approaching the receiver line with a significant azimuthal angle making an example of the OP type (Figure 1b). Furthermore, source points on the surveying road can be close to the array (for example, at a distance shorter than a few times array length from either end or even within the receiver line), making an example of the OC type (Figure 1c). Waves of OC type propagate into the receiver line with a significant curvature due to the proximity and the offline nature. A considerable amount of recorded energy can be of this origin due to the proximity of the source points.

The IP waves will make a straight linear arrival pattern on the recorded data with a slope ($S= dt/dx$) the same as the inverse of the phase velocity ($1/c$) (i.e., slowness) for a particular frequency (f) (Figure 2). The OP waves will also make a straight linear arrival pattern but with its slope always smaller than that ($1/c$) of the IP case by a ratio of cosine of the azimuth ($\cos\theta$) (Park et al., 2004). Then, its corresponding velocity (dx/dt) will be overestimated by a ratio of $1/\cos\theta$ if the offline nature is not properly accounted for. The arrival pattern of the OC waves will be hyperbolic with an asymptote the same as that of the OP for the same azimuth (θ).

Schemes for Dispersion Imaging

Dispersion imaging schemes to deal with each of these types of propagation are described. It is assumed that the road runs along the horizontal axis (x) with the receiver line in parallel to it with a certain vertical separation (dy) (Figure 3).

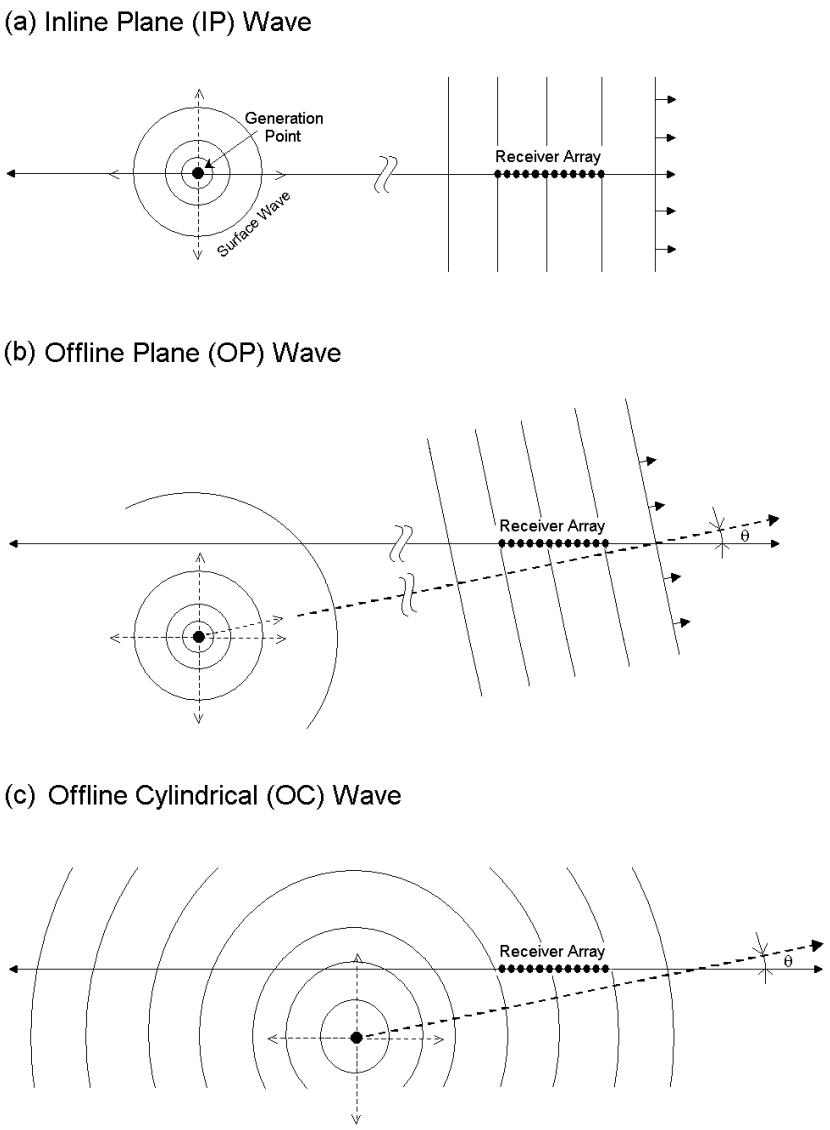

Figure 1. Three different types of possible wave propagation with a roadside surface wave method employing a 1D linear receiver array parallel to road.

Inline Plane (IP) Waves

IP waves are the simplest type from the data processing perspective. They can be processed by any scheme commonly used for active surveys. With the scheme by Park et al. (1998; 2004), to calculate the relative energy, $E_{IP}(\omega,c)$, for a particular frequency ($\omega=2\pi f$) and a scanning phase velocity (c) in the dispersion image, it first applies the necessary phase shift ($\phi_i=\omega x_i/c$) to the Fourier transformation, $R_i(\omega)$, of the *i-th* trace, $r_i(t)$, at offset x_i, sums all (N) phase-shifted traces, and then takes the absolute value of the summed complex number:

$$E_{IP}(\omega,c)=\left|\sum_{i=1}^{N} e^{j\phi_i} R_i(\omega)\right|+\left|\sum_{i=1}^{N} e^{-j\phi_i} R_i(\omega)\right| \qquad (1)$$

To account for the possible bidirectional nature of the incoming waves from both ends of the receiver array, the step of phase shift followed by the summation is repeated by changing the sign of the phase shift in the above equation. A method by Louie (2001)—commonly known as the refraction microtremor (ReMi) method—is based on this algorithm by assuming that the major part of the recorded waves are of IP type and any other offline waves of significant energy, if they exist, should appear at higher phase velocities. It therefore tries to extract a curve by following a trend of lowest phase velocity in the energy band of dispersion in the space of $E_{IP}(\omega,c)$. With this method, however, the consideration of the inherent banding effect due to the limited spatial coverage of the measurement is not properly accounted for.

Figure 4 shows processing results obtained by using the above equation (1) when applied to synthetic 24-channel records generated from an inline source (S0) marked in Figure 3. A dispersion curve with an arbitrary constant phase velocity of 500 m/sec was used during the modeling. The effect of using different receiver array lengths is also shown. This modeling with a perfectly inline source illustrates the inherent band appearance of the image resulting from a processing scheme applied to finite lengths in time (t) and space (x). Width of the band also changes with wavelength as well as length of the receiver line.

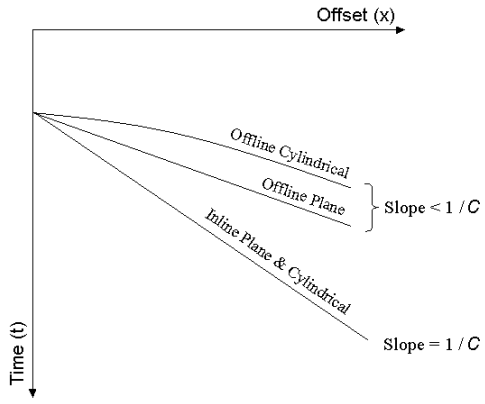

Figure 2. A schematic showing arrival patterns of different types of wave propagation as appearing in offset (x) and time (t) space.

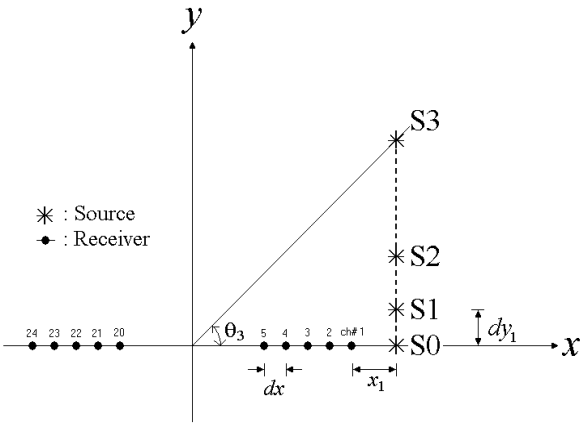

Figure 3. A relative coordinate system considering a linear receiver array and source points of different offline angles.

Offline Plane (OP) Waves

OP waves can be processed by any algorithm based on the conventional 2D wavenumber (k_x-k_y) method (Lacoss et al., 1969; Capon, 1969). The method by Park et al. (2004) modifies the traditional method in such a way that the possible multi-modal nature of dispersion can be imaged in an intuitive manner by stacking energy in the 2D wavenumber space along the azimuth axis. This method therefore adds another parameter for scanning in comparison to (1): the azimuth (θ). For each frequency (ω), the energy, $E_{OP}(\omega,c,\theta)$, for a scanning phase velocity (c) is calculated by assuming an azimuth (θ). This calculation is then carried over the scanning range of the phase velocity (for example, 50 m/sec-3000 m/sec with 5-m/sec increment), and then over that of the azimuth (for example, 0-180 degrees in 5-degree increments):

$$E_{OP}(\omega,c,\theta)=\left|\sum_{i=1}^{N} e^{j\phi_{\theta,i}} R_i(\omega)\right| \quad (\text{for } 0^\circ \le \theta \le 180^\circ) \tag{2}$$

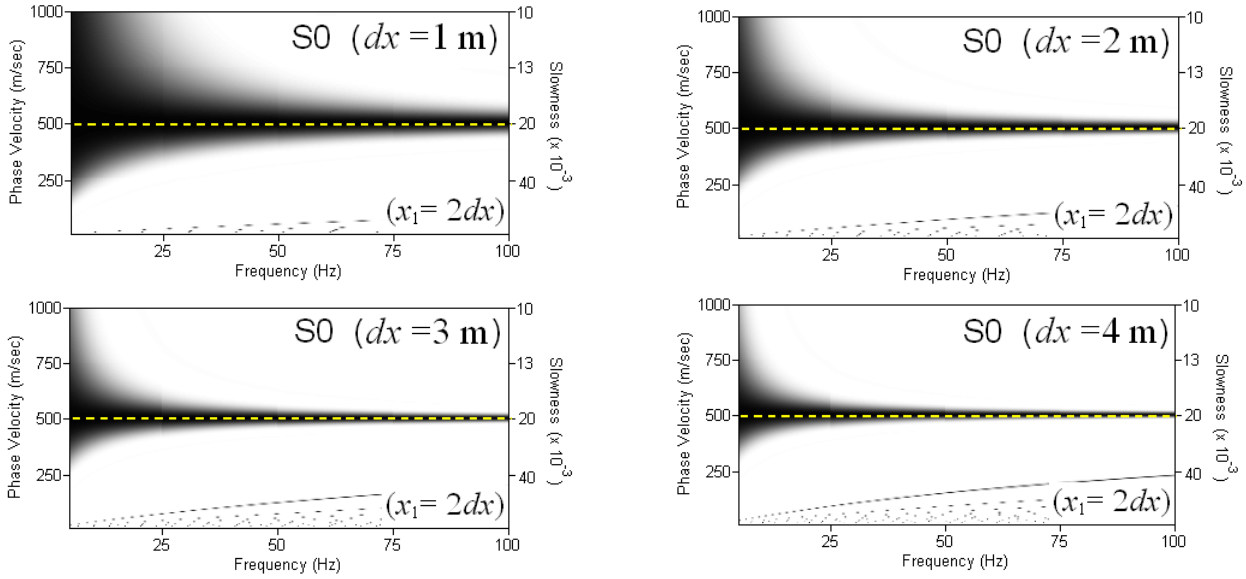

Figure 4. Dispersion images processed from synthetic records modeling a perfectly inline source (S0) in Figure 3 obtained by using the inline plane (IP) wave processing scheme. Four different receiver intervals (*dx's*) were used in the modeling to consider different receiver array lengths.

For given c and θ, the necessary phase shift $\phi_{\theta,i}$=-$\omega x_i \cos\theta/c$ for a trace at x_i is calculated based on the projection principle (Park et al., 2004). Here the scanning range of azimuth (θ) is only within the two quadrants (180 degrees) due to the linear nature of the receiver line. All the IP waves that exist are handled in a correct manner as they are detected during the scanning of azimuth near 0 and 180 degrees, respectively.

Offline Cylindrical (OC) Waves

OC waves are processed in a similar manner to the OP waves, (2), only with an additional consideration of the finite, rather than infinite, distance ($l_{\theta,i}$) between the source point (x_θ, y_θ) and each receiver point (x_i) for a scanning angle θ (Figure 5):

$$l_{\theta,i} = \sqrt{(x_\theta - x_i)^2 + y_\theta^2} \quad (\text{with } x_\theta = y_\theta / \tan\theta \text{ and } y_\theta = dy) \tag{3}$$

Then, the phase shift term in equation (2) is determined as $\phi_{\theta i}$=-$\omega l_{\theta,i}/c$. The distance, $l_{\theta i}$, obviously can change as the road itself has its own width and irregularities may exist anywhere on the road. An extensive modeling experiment indicated that the exact distance, however, is not critical and that the distance between the center of the road and the receiver line is usually sufficient enough to account for the curvature in the arrival pattern of the OC waves. This scheme processes the IP waves correctly as it becomes identical to that for the IP waves for grazing azimuthal angles (close

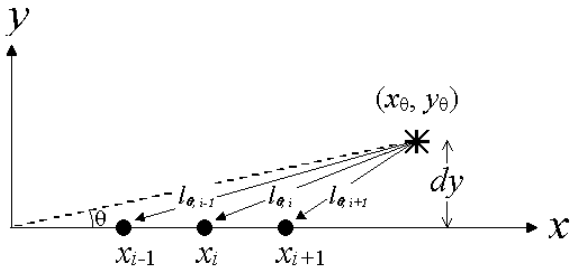

Figure 5. A schematic illustration of how the offline cylindrical waves are accounted for during the scanning of an azimuth (θ).

to 0 or 180 degrees). OP waves (for example, waves from other nearby roads) can also be processed by this scheme, only with a slightly reduced sensitivity.

Synthetic Data Testing of Offline Schemes

All these three schemes are tested on synthetic data sets. A modeling scheme introduced in Park and Miller (2005) was used to generate synthetic records (not shown) of 24-channel acquisition with a linear receiver array of 2-meter spacing (Figure 3). Three different source points (S1, S2, and S3) were separately modeled that had azimuths of θ=15°, 30°, and 45° with the same inline offset (x_1). A constant phase velocity of 500 m/sec was used for a frequency band of 5-100 Hz. Attenuation of near-surface materials was accounted for by including a Q-factor of 30 as a frequency-dependent energy modulation factor of surface waves in addition to the cylindrical divergence term. Although all the modeled source points were offline, the inline processing scheme of (1) was also applied for a comparison purpose. Figure 6 shows processing results from all these schemes. The modeled phase velocity of 500 m/sec has been indicated by a straight dotted line in the figures. Those curves extracted from the amplitude peaks in the dispersion images also have been superimposed.

Results from the IP scheme show the imaged phase velocities being progressively higher as the azimuth of source point increases (Figures 6a-6c). For relatively large azimuths (θ = 30° and 45°), the image trend converges to the theoretical value ($=c/\cos\theta$) at higher frequencies (> 50 Hz), whereas it tends to deviate more at lower frequencies. This non-constant nature of the deviation is due to the proximity of source points in comparison to total length of the receiver array. Performance of the OP scheme (Figures 6d-6f) shows a lesser degree of overestimation, indicating a correction capacity in comparison to the IP scheme. The results from the OC scheme (Figures 6g-6i) show the least amount of overestimation for all three source points. None of the three schemes, however, shows complete results without any deviation from the correct value. The most accurate estimation is obtained through a survey using a true 2D receiver array followed by data processing using the OP scheme (Figure 7).

Relative performance of the OC scheme is maximized when the *x*-coordinate of a source point is within that of the receiver line (infraline case) as noticed from another modeling example illustrated in Figure 8. Figure 9 shows the performance results from a modeling of multiple source points with the same offline distance (*dy*) of 10 meters. It is noted that the OC scheme gives the most accurate results, whereas results from the IP scheme show the largest deviation in general trend of the image. Results from intensive modeling indicated that the OP and OC schemes tend to produce less deviation when multiple sources are modeled than with the single-source case displayed in Figure 6.

Field Data Example

Two sets of field data were used to test these three processing schemes. One data set (OCT-03) was prepared from the data set acquired in October 2003 (Park et al., 2004) near a soccer field in Lawrence, Kansas, by using a 2D cross layout of total 48 channels (Figure 10) with a 5-m receiver spacing. The first 24-channel data that ran East-West (E-W) in parallel to the Clinton Parkway were taken to mimic a 1D linear array. The separation (*dy*) between this receiver line and the center of Clinton Parkway was about 100 meters. For comparison purposes, a dispersion image and its corresponding curve that were obtained from the full data set of the 2D cross layout have been displayed in Figure 10b. The other set of data (OCT-05) was acquired in October 2005 using a 24-channel linear array directly south of the E-W line used for OCT-03 by using the same receiver spacing of 5 meters (Figure 10). This line was about 30 meters from the road (*dy* = 30 m).

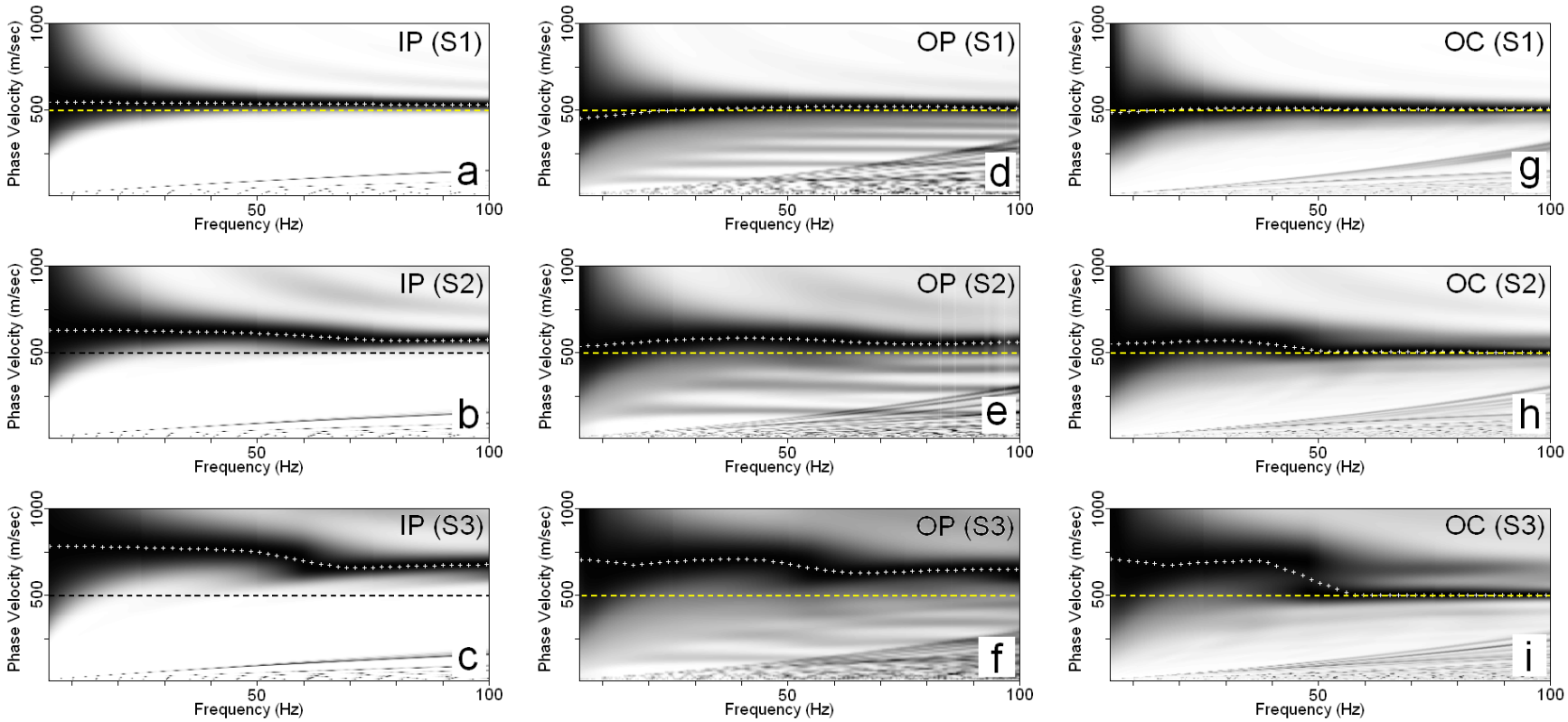

Figure 6. Dispersion images processed from synthetic records modeling three different offline sources (S1, S2, and S3) marked in Figure 3 by using three different processing schemes: inline plane (IP), offline plane (OP), and offline cylindrical (OC) schemes. The modeled phase velocity of 500 m/sec is indicated by a straight dotted line on each image, and trends of the energy peaks in each image are visible by cross marks superimposed on top of the major energy bands.

Ten individual records acquired at each survey time were processed using three different schemes, and their dispersion images were vertically stacked together (to increase the image resolution) to make the images displayed in Figures 11-12. The strong major trend of dispersion visible on all images in 8-17 Hz was previously confirmed as a higher mode (M1), instead of the fundamental mode (M0), through a combined analysis with an active survey (Park et al., 2005). Dispersion curves were extracted from the trends by picking maximum points in the energy band with a small interval (0.01 Hz) and then calculating the best fitting curve through the linear regression method. All these curves are displayed in Figures 11d and 12d. Curves from the IP scheme show overestimations in comparison to those from the other two schemes in both surveys. The amount of overestimation, however, becomes smaller as the receiver array gets closer to road. It is also shown that the two offline (OP and OC) schemes resulted in a certain amount of overestimation for frequencies lower than 12 Hz (for wavelengths longer than about 75 meters) as noticed when compared to the curve from a 2D cross layout. Curves from the survey closer to the road show (OCT-05) a slight difference in general trend, possibly due to a slight difference in near-surface geology in comparison to the results from the previous survey performed about 70-meters further away.

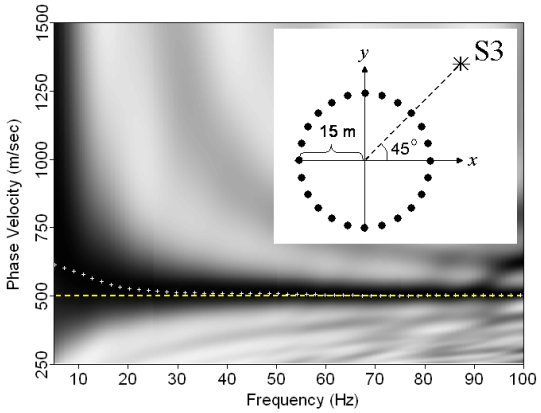

Figure 7. Dispersion image of the synthetic 24-channel record modeling the offline source S3 with a 2D circular array (inset). The offline plane (OP) scheme was used to process the data.

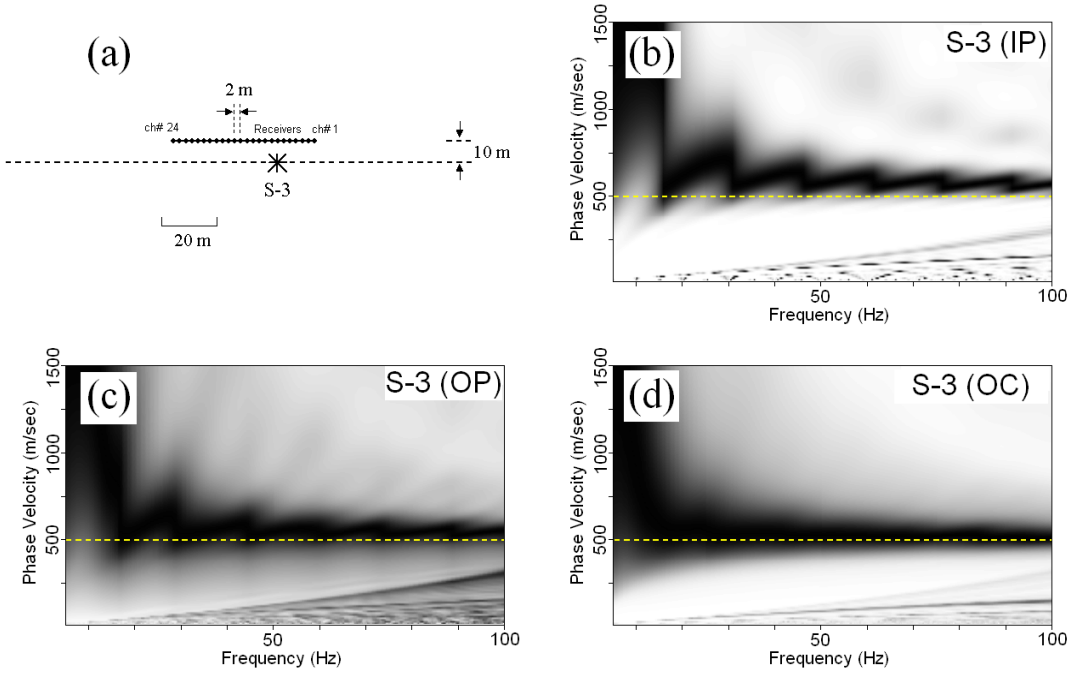

Figure 8. (a) A schematic showing the relative locations of the receiver array and an offline source (S-3) used to generate a 24-channel synthetic record. Dispersion images processed from the record by using (b) inline plane (IP), (c) offline plane (OP), and (d) offline cylindrical (OC) schemes.

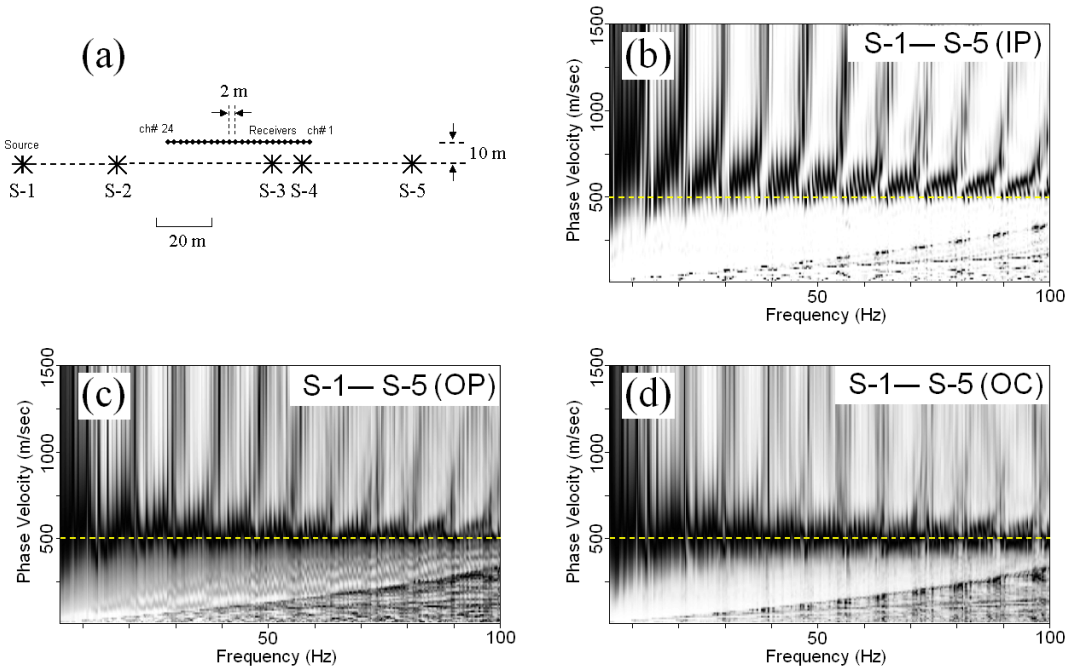

Figure 9. (a) A schematic showing relative locations of the receiver array and five offline sources (S-1 through S-5) simultaneously modeled to generate a synthetic 24-channel record. Dispersion images processed from the record by using (b) inline plane (IP), (c) offline plane (OP), and (d) offline cylindrical (OC) schemes.

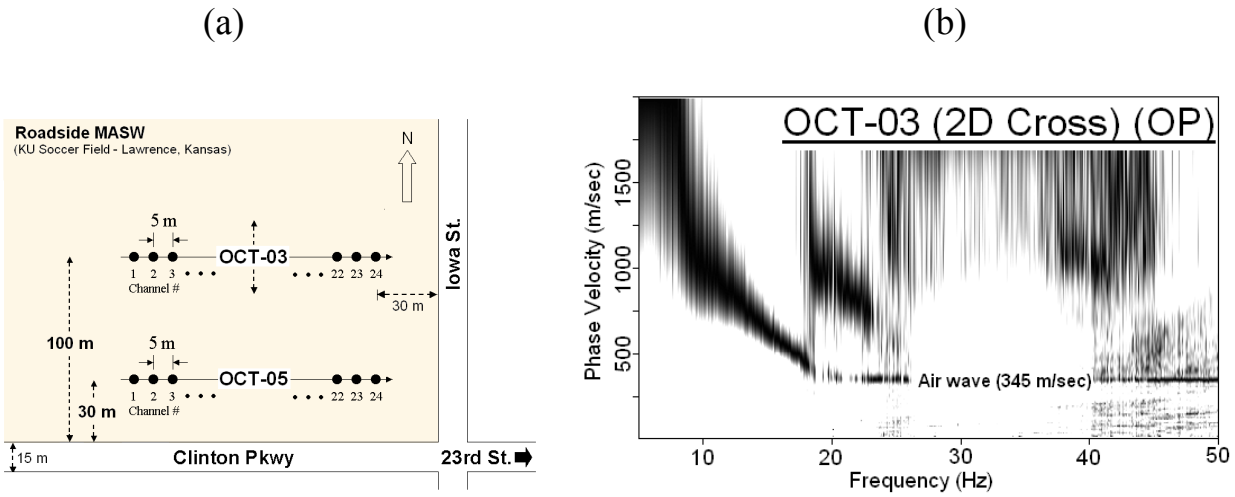

Figure 10. (a) Map showing field layouts for two experiments performed during October of 2003 (OCT-03) and 2005 (OCT-05). A 48-channel 2D cross receiver array was used for the earlier experiment. (b) Dispersion image processed from the 48-channel 2D array records by using the offline plane (OP) scheme.

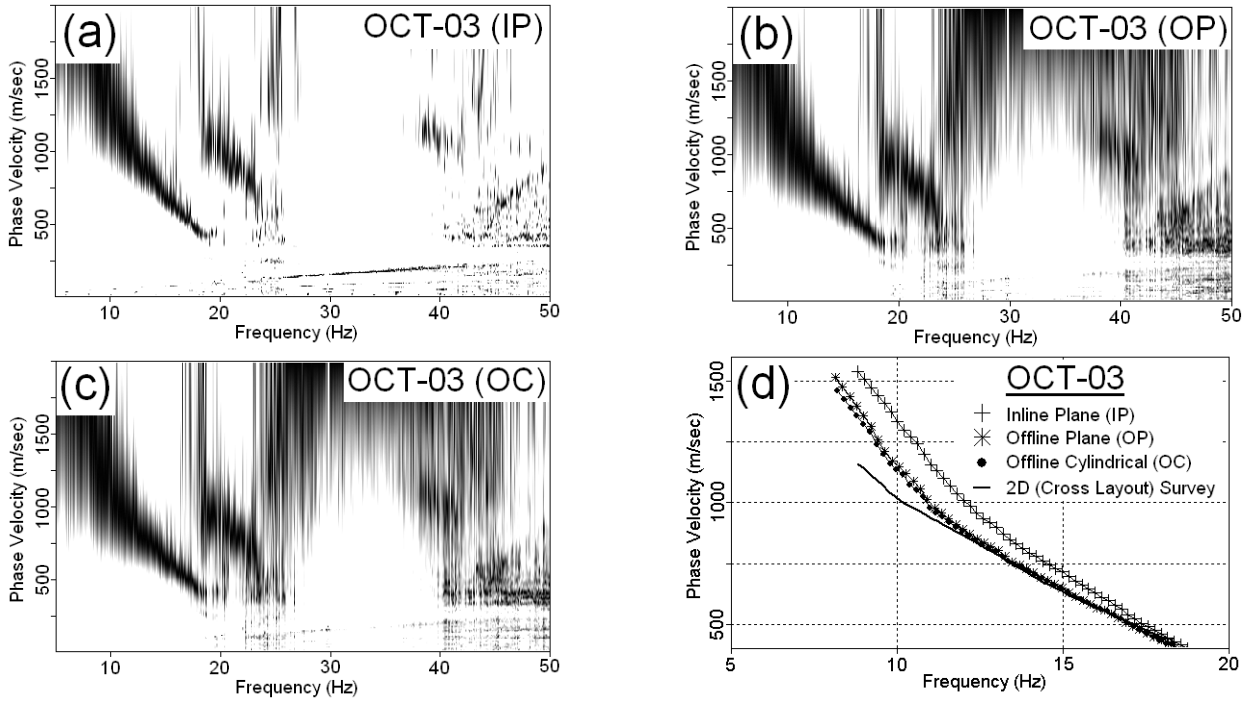

Figure 11. Dispersion images processed from 24-channel records along the E-W line used during the field experiment in October 2003, obtained by using (a) inline plane (IP), (b) offline plane (OP), (c) offline cylindrical (OC) schemes, and (d) curves extracted from the major energy trend.

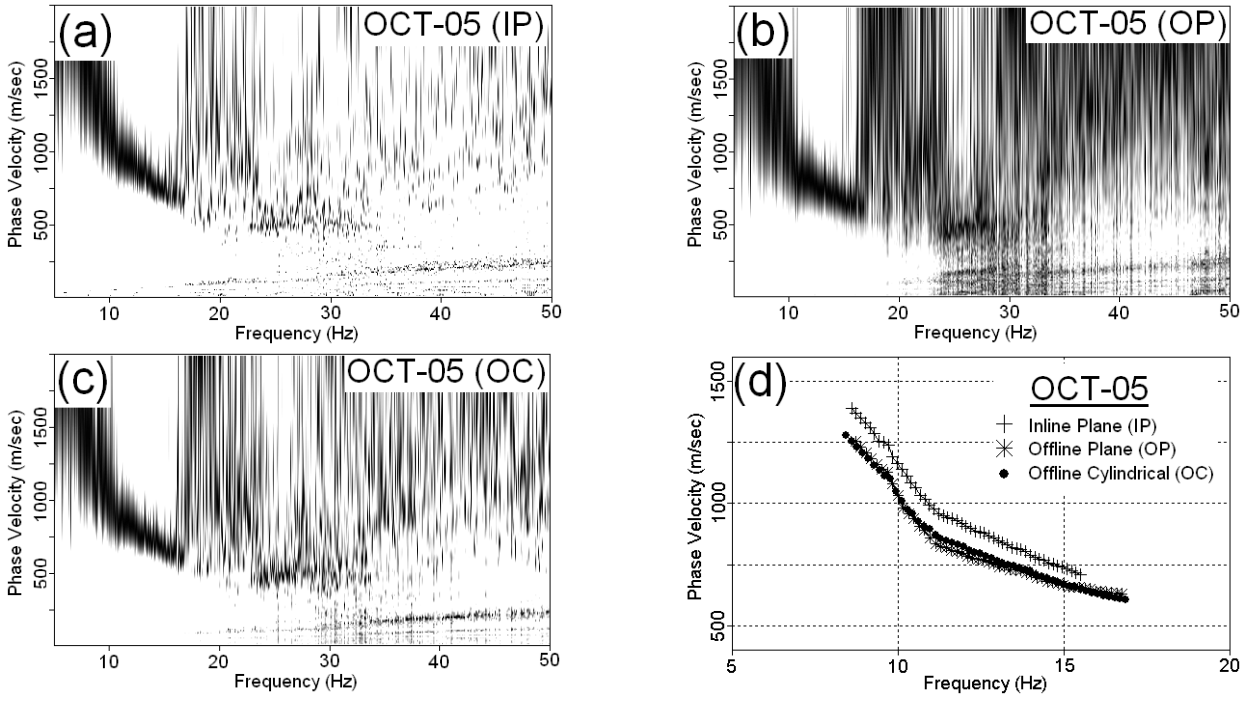

Figure 12. Dispersion images processed from 24-channel linear array used during the field experiment in October 2005, obtained by using (a) inline plane (IP), (b) offline plane (OP), (c) offline cylindrical (OC) schemes, and (d) curves extracted from the major energy trend.

Discussions

It was shown through numerical modeling that the OC scheme should give a superior performance especially when there are some infraline source points on the road. Field data examples did not demonstrate this point, as the results from both OP and OC schemes were almost identical. This indicates that there were not such strong infraline source points on the road at the particular location where the surveys were performed. Azimuthal analysis for major source points in the surveyed area performed with the 2D (cross and circular) receiver layouts (Park et al., 2004; Park and Miller, 2005) indicated that major contribution of surface waves came from the 23rd St. close to the intersection with the Iowa St.

Because the relative dominance of each type of waves cannot be known in advance, using the OC scheme is recommended if the road is fairly straight for a significant distance without any other major roads intersecting or passing nearby. The OP scheme may also be applied for comparison purposes. The IP scheme can be a convenient tool for a quick in-field quality control purpose, as it is the fastest scheme.

The uneven nature of wavelengths near the source point can be accounted for in the OC scheme by using the Hankel function (Zywicki, 1999). Its significance will be presented in future publications after testing with modeling and field data acquired with both 1D and 2D layouts.

Even if a 2D layout and the subsequent OP scheme are used, overestimation can still be significant for those long wavelengths comparable to distance to the major source points as seen from the modeling result shown in Figure 7. This finite (instead of infinite) nature of the source distance is inherent to the passive surface wave methods utilizing local traffic noise. The OC scheme was applied only to the linear array, but it can be extended to a 2D layout. Testing results of this extension will be presented in future publications.

Conclusions

With a roadside surface wave survey using a linear receiver array, using a 2D dispersion analysis scheme (despite the 1D nature of data acquisition) that accounts for the offline nature of the passive surface waves is recommended. In addition, considering a relatively long receiver array and the possibility of strong surface waves being generated at nearby points on the road, accounting for the cylindrical nature through a simple modification of the 2D algorithm to improve the accuracy of the processing is also recommended.

Acknowledgments

Field experiments were made through careful preparations and precise operations performed by Brett Wedel, Noah Stimac, Larry Waldron, and Brett Bennett at the Kansas Geological Survey (KGS). We give our sincere appreciation to them. We also thank Marla Adkins-Heljeson and Mary Brohammer at KGS for their helps with the manuscript preparation.

References

Capon, J., 1969, High resolution frequency-wavenumber analysis: Proc. Inst. Elect. and Electron Eng., **57**, 1408-1418.

Haruhiko, H., and Hayashi, K., 2003, Shallow S-wave velocity sounding using the microtremors array measurements and the surface wave method; Proceedings of the SAGEEP 2003, San Antonio, TX, SUR08, Proceedings on CD ROM.

Lacoss, R.T., Kelly, E.J., and Toksöz, M.N., 1969, Estimation of seismic noise structure using arrays: Geophysics, **34**, 21-38.

Louie, J.N., 2001, Faster, better: shear-wave velocity to 100 meters depth from refraction microtremor arrays; Bulletin of the Seismological Society of America, 2001, **91**, (2), 347-364.

Okada, H., 2003, The microtremor survey method; Geophysical Monograph Series, no. 12, published by Society of Exploration Geophysicists (SEG), Tulsa, OK.

Park, C.B., Miller, R.D., Ryden, N., Xia, J., and Ivanov, J., 2005, Combined use of active and passive surface waves: *Journal of Engineering and Environmental Geophysics (JEEG)*, **10**, (3), 323-334.

Park, C.B., Miller, R.D., Xia, J., and Ivanov, J., 2004, Imaging dispersion curves of passive surface waves: SEG Expanded Abstracts: Soc. Explor. Geophys., (NSG 1.6), Proceedings in CD ROM.

Park, C.B. and Miller, R.D., 2005, Multichannel analysis of passive surface waves — modeling and processing schemes: Proceedings of the *Geo-Frontiers* conference, Austin, Texas, January 23-26, 2005.

Park, C.B., Miller, R.D., and Xia, J., 1999, Multichannel analysis of surface waves (MASW); Geophysics, **64**, 800-808.

Park, C.B., Xia, J., and Miller, R. D., 1998, Imaging dispersion curves of surface waves on multi-channel record; SEG Expanded Abstracts, 1377-1380.

Yoon, S., and Rix, G., 2004, Combined active-passive surface wave measurements for near-surface site characterization; Proceedings of the SAGEEP 2004, Colorado Springs, CO, SUR03, Proceedings on CD ROM.

Zywicki, D.J., 1999, Advanced signal processing methods applied to engineering analysis of seismic surface waves: Ph.D. thesis, Georgia Institute of Technology.